

# Melatonin affects hypoxia-inducible factor 1 $\alpha$ and ameliorates delayed brain injury following subarachnoid hemorrhage via H19/miR-675/HIF1A/TLR4

## Da-yong Xia

Department of Neurosurgery, The First Affiliated Hospital of Wannan Medical College, Wuhu 241000, Anhui Province, People's Republic of China.

## Xiao-chun Jiang

Department of Neurosurgery, The First Affiliated Hospital of Wannan Medical College, Wuhu 241000, Anhui Province, People's Republic of China.

## Zhen-bao Li

Department of Neurosurgery, The First Affiliated Hospital of Wannan Medical College, Wuhu 241000, Anhui Province, People's Republic of China.

## Yi Dai

Department of Neurosurgery, The First Affiliated Hospital of Wannan Medical College, Wuhu 241000, Anhui Province, People's Republic of China.

## Zi-huan Zhang

Department of Neurosurgery, The First Affiliated Hospital of Wannan Medical College, Wuhu 241000, Anhui Province, People's Republic of China.

## Song Yang (✉ [melatoninsah@yeah.net](mailto:melatoninsah@yeah.net))

Yantai Ludong Hospital

---

## Research

**Keywords:** Melatonin, TLR4, HIF1A, DBI following SAH, H19, miR-675, apoptosis

**Posted Date:** February 26th, 2020

**DOI:** <https://doi.org/10.21203/rs.2.24591/v1>

**License:**  This work is licensed under a Creative Commons Attribution 4.0 International License.

[Read Full License](#)

---

# Abstract

**Background:** This study was aimed to investigate the molecular mechanism of how melatonin interferes with hypoxia-inducible factor 1 $\alpha$  (HIF1A) and TLR4 expression, which is implicated in the management of delayed brain injury (DBI) after subarachnoid hemorrhage (SAH).

**Method:** Luciferase assay, real-time PCR, Western-blot analysis and immunohistochemistry (IHC) assays were utilized to explore the interaction among H19, miR-675, HIF1A and TLR4, and to evaluate the effect of MT on the expression of above transcripts in different groups.

**Results:** MT enhanced H19 expression by promoting the transcription efficiency of H19 promoter, and HIF1A was identified as a target of miR-675. HIF1A enhanced TLR4 expression via promoting the transcription efficiency of TLR4 promoter. Furthermore, administration of MT up-regulated miR-675 but suppressed the expressions of HIF1A and TLR4. Treatment with MT alleviated neurobehavioral deficits and apoptosis induced by SAH. According to the result of IHC, HIF1A and TLR4 protein levels in the SAH group were much higher than those in the SAH+MT group. Therefore, the administration of MT increased the levels of H19 and miR-675 which have been inhibited by SAH. In a similar way, treatment with MT decreased the levels of HIF1A and TLR4 which have been enhanced by SAH.

**Conclusion:** MT could down-regulate the expression of HIF1A and TLR4 via the H19/miR-675/HIF1A/TLR4 signaling pathway, while TLR4 is crucial to the release of pro-inflammatory cytokines. Therefore, the treatment with MT could ameliorate post-SAH DBI.

## Introduction

Subarachnoid hemorrhage (SAH) is a disease in which the arterial blood flow points to the direction of subarachnoid space in the brain. The most frequent cause of SAH is ruptured aneurysm. SAH is a serious disorder with an annual incidence of 6–7 per 100,000 people and high mortality of 50% [1]. Treatment for SAH has primarily focused on the prevention of bleeding in the intracranial aneurysm, a factor contributing to early brain injury (EBI), as well as on the reversal of cerebral vasospasm, a critical cause of delayed brain injury (DBI) [2]. In fact, DBI and delayed cerebral ischemia following EBI are still considered as the most critical and preventable causes of poor prognosis in SAH, whereas inflammation has been considered as the key factor affecting the severity of brain injury [3].

Toll-like receptor 4 (TLR4) is highly expressed in the brain and can be activated by extravasated blood and damaged brain tissues upon the rupture of an intracranial aneurysm [4]. The inflammatory reaction and tissue damages caused by SAH can further activate TLR4, thus leading to EBI [3]. Previous studies have mainly concentrated on the role of the TLR4/nuclear factor kappa B (NF- $\kappa$ B) pathway in EBI, although no specific TLR4 antagonists have ever been tested for EBI [5]. After the stimulation of TLR4 with ligands, the myeloid differentiation factor 88 (MyD88)-dependent pathway can activate the nuclear factor (NF)- $\kappa$ B and synthesize pro-inflammatory cytokines or factors, including tumor necrosis factor (TNF)- $\alpha$ , interleukins such as IL-12, IL-8, IL-6 and IL-1 $\beta$ , matrix metalloproteinase (MMP)-9, intercellular

adhesion molecule (ICAM)-1, cyclooxygenases, superoxide, monocyte chemo-attractant protein (MCP)-1, nitric oxide and hydrogen peroxide [6].

As a type of small non-coding RNAs, miRNAs play an essential role in gene regulation [7]. In fact, multiple roles of miRNA have been discovered in a wide range of physiological processes such as apoptosis, cell differentiation, cell growth, and carcinogenesis [8]. On the other hand, long non-coding RNAs (lncRNAs) are transcripts of more than 200 nt in length and are implicated in various critical cellular functions, such as RNA processing, chromatin modification, and gene regulation [9]. Previous articles have demonstrated that H19 expression is substantially increased upon cerebral I/R injury [10]. It has also been demonstrated that H19 can regulate post-SAH brain injury by mediating NGF- and P53-induced apoptosis through let-7a and microRNA - 675 [11].

As a pharmacologic agent and a powerful antioxidant, melatonin (MT) can pass through the blood-brain barrier (BBB) easily and is associated with minimal toxicity even if it is consumed in large doses [12]. MT has been demonstrated to exert neuroprotective effects in animals suffering from neurologic injuries, including ischemic stroke and traumatic brain injury [13, 14]. MT has been found to up-regulate the expression of H19, whereas miR-675 is located within the chromosomal segment of H19 [15, 16]. Moreover, patients suffering from post-SAH EBI was found to typically experience abnormally enhanced inflammatory response, oxidative stress, cerebral vasospasm, and cell death [17], and a study by Yang et al., also demonstrated that MT treatment could substantially attenuate the neurological deficits while reducing the brain swelling in post-SAH EBI [18, 19].

Furthermore, hypoxia-inducible factor 1 $\alpha$  (HIF1A) was found to be a target gene of miR-675 and could induce the expression of TLR4. Therefore, HIF1A may regulate the expression of miR-675 [20]. Based on the above-mentioned evidence, we postulated that the signaling pathway of H19/miR-675/HIF1A/TLR4 might mediate the therapeutic effect of MT in the management of post-SAH DBI. To test such hypothesis, we established an animal model of SAH and treat it with MT. Subsequently, we investigated the involvement of the H19/miR-675/HIF1A/TLR4 signaling pathway in the effect of MT on the management of post-SAH DBI.

## **Materials And Methods**

### **Animals**

A total of 36 adult male C57BL/6J mice between ten to twelve weeks old were used in this study. These mice were purchased from the experimental animal center of our institute and weighed between 22 and 25 g. All experiments were carried out under NIH's Guide for the Care and Use of Laboratory Animals and were approved by the Ethics Committee of Yantai Ludong Hospital (Code: 160688M001).

### **SAH Model**

An endovascular perforation method was used to establish the animal model of SAH as previously described [21, 22]. In brief, 50 mg/kg pentobarbital sodium was injected to carry out anesthetization. A heat blanket was then used to maintain the rectal temperature of mice at  $37 \pm 0.5$  °C. The internal carotid artery, external carotid artery and left common carotid artery were then exposed through a midline incision at the neck, followed by ligation and dissection at the left external carotid to leave a 3-mm stump. A 5-0 nylon suture was then inserted into the left internal carotid artery to perforate the artery at the bifurcation of the anterior and middle cerebral arteries. The identical procedures were performed on sham-operated mice except for the artery perforation.

## **Experimental Protocol**

The mice were assigned into the groups listed below: (1) SAH group (n= 12), (2) sham group (n= 12), (3) SAH + MT group (n= 12). For the MT group, MT was dissolved in 1% ethanol in 1 mL sterile saline, then intraperitoneally injected at a dose of 150 mg/kg and 12 h after SAH [23].

## **Neurological Score**

Neurological deficits were evaluated at 96h after the onset of SAH using an 18-point system containing six tests per previous published protocol [22, 24]: forelimbs outstretching (0–3), spontaneous activity (0–3), climbing (1–3), symmetry in the movements of all limbs (0–3), response to vibrissae touch (1–3) and body proprioception (1–3). A higher score indicates an elevated function.

## **Brain Water Content**

The standard wet-dry method was used to measure the brain water content in each mouse. In brief, the mice were sacrificed 96h post-operation to have their brains immediately isolated and separated into the right and left cerebellum, cerebral hemispheres and brain stem. These brain parts were weighed respectively to obtain their wet weight. Subsequently, the brain sections were dried for 24 hours at 105°C and weighed to obtain the dry weight. Finally, the brain water content was calculated as (wet weight - dry weight)/wet weight× 100%.

## **RNA isolation and real-time PCR**

Tissue and cell samples were treated with TRIZOL (Invitrogen, Carlsbad, CA) to extract total RNA, which was then converted to cDNA on a PE9600 PCR instrument (Perkin-Elmer, Foster City, CA). The mRNA expression of H19, miR-675, HIF1A, and TLR4 was then measured using real-time PCR using an SYBR Green kit following the manufacturer's instructions. Accordingly, U6 and GAPDH were used as internal control. The thermocycle conditions were: 95°C for 5 min, 45 cycles of 95°C for 10s and 60°C for 50s, 90°C for 1 min, 55°C for 1 min, 95°C for 30s. All experiments were repeated in triplicated and the data was analyzed by the  $2^{-\Delta\Delta C_t}$  method [25]. The primers pairs used were: H19-forward: 5'-TGCTGCACTTTA CAACCACTG-3'; H19-reverse: 5'- ATGGTGTCTTTGATGTTGGGC-3'; miR-675-forward: 5'- TGGTGC GGAGAGGGCCACAGTG-3'; miR-675-reverse: 5'-GCGAGCACAGAATTAATACGAC-3'; HIF1A-forward: 5'-CGTGTTATCTGTCGCTTTGAGTC-3'; HIF1A-reverse: 5'-GTCTGGCTGCTGTAATAATGTTCC-3';

TLR4-forward: 5'-GGCATCATCTTCATTGTCCTTG-3'; TLR4-reverse: 5'-AGCATTGTCCTCCCACTCG-3'; U6-forward: 5'-CGCTTCGGCAGCACATACTA-3'; U6-reverse: 5'-CGCTTCACGAATTTGCGTGTCA-3'; GAPDH-forward: 5'-CTTTGTCAAGCTCATTTCTGG-3', GAPDH-reverse: 5'-TCTTGCTCAGTGTCTTGC-3'.

## **Cell culture and transfection**

U251 and SH-SY5Y cells were cultured at 37°C and in 95% humidity and 5% CO<sub>2</sub> with a Dulbecco's modified eagle medium (DMEM) (Invitrogen, Carlsbad, CA) containing 10% fetal calf serum (FCS) (Invitrogen, Carlsbad, CA). When the cultured cells grew to 90% adherence, they were passaged. Subsequently, the cell transfection was accomplished using Lipofectamine 2000 following the instruction of the manufacturer. For MT treatment, the cells were treated with 1 µm and 5 µm of MT for 48 h before the cells were collected for subsequent analyses [23].

## **Luciferase assay**

Full length 3' UTR of HIF1A was amplified by PCR and cloned into a pGL3 vector (Promega, Madison, WI) downstream of the firefly luciferase reporter gene. Subsequently, a Quick-change site-directed mutagenesis kit (Stratagene, La Jolla, CA) was used to generate mutated 3' UTR of HIF1A, which was also inserted to a pGL3 vector and used for subsequent transfection experiments. Similarly, miR-675 mimics were designed and synthesized before they were co-transfected to U251 and SH-SY5Y cells with either wild type (WT) or mutated 3' UTR of HIF1A. At 48 h after transfection, the cells were harvested and the luciferase activity in transfected cells was measured using a dual-luciferase reporter assay (Promega, Madison, WI). In order to investigate the effect of HIF1A on the promoter of TLR4, the full length of TLR4 promoter was amplified by PCR and cloned into the pGL3 vector. Subsequently, HIF1A and TLR4 promoter were co-transfected to U251 and SH-SY5Y cells. At 48 h after transfection, the cells were harvested and the luciferase activity in transfected cells was measured using the dual-luciferase reporter assay.

## **Western blot analysis**

Tissue samples (basal cortical samples) were pooled and cell samples were lysed and resolved using 12% SDS-PAGE. Subsequently, the resolved proteins were blotted onto a membrane, which was then blocked at room temperature for 1 h with Tris-Buffered Saline and Tween 20 (TBST) containing 5% bovine serum albumin (BSA) and incubated at 4°C overnight with primary antibodies against HIF1A (ab92498, Abcam, Cambridge, MA) and TLR4 (ab8378, Abcam, Cambridge, MA). After TBST washing, the membrane was further incubated for 1h at 37°C with HRP-labeled second antibodies (ab6728, Abcam, Cambridge, MA). Finally, after being developed using chemiluminescence reagents (Santa Cruz Biotech, Santa Cruz, CA), the optical density values of target proteins were measured.

## **Apoptosis analysis**

Treated U251 and SH-SY5Y cells were harvested by centrifugation. Subsequently, the cells were suspended in PBS to a concentration of 5-10 × 10<sup>4</sup> cells/mL and incubated with Annexin V-FITC and

Propidium iodide. In the next step, the cell apoptosis profiles in different groups were analyzed using a FACSCanto II flow cytometer (BD, Franklin Lakes, NJ). The final apoptosis rate = early apoptosis rate + late apoptosis rate.

### **Immunohistochemistry assay**

Histochemical immunostaining assay was done using a streptavidin-peroxidase (SP) three-step method. All samples were first fixed in 4% formalin and embedded in paraffin. After antigen repair, the slides were incubated overnight at 4°C with primary antibodies against HIF1A (ab92498, Abcam, Cambridge, MA) and TLR4 (ab8378, Abcam, Cambridge, MA). After being washed repeatedly with PBS, the slides were incubated for 10 min at room temperature with the secondary antibody. Subsequently, the reaction was terminated by an anti-biotin-labeled peroxidase solution, and the slides were colorized with DAB. After restaining with hematoxylin, the slides were dehydrated with anhydrous ethanol and dried before they were mounted in neutral gum and observed under a microscope.

### **TUNEL assay**

The frozen tissue samples were recovered at room temperature for 5-10s, followed by the addition of a resuscitation solution. After resuscitation, the samples were stained using a TUNEL kit (Beyotime, Shanghai, China). Subsequently, the samples were immersed in a 3% H<sub>2</sub>O<sub>2</sub> solution at room temperature for 10 min and then rinsed with PBS for 5 min. After the addition of 50 µL of proteinase K solution (20 µg/mL), the samples were hydrolyzed for 20 min at room temperature to remove tissue proteins. On the next, the samples were washed with PBS and the antigen retrieval was done using a citrate buffer (0.01 M). Subsequently, the sections were cooled to room temperature and washed with PBS. Then, 50 µL of a TdT enzyme solution was added to the slices and incubated at 37 °C for 1 h, whereas the reaction solution containing no TdT enzyme was used as a negative control. After the slices were washed with PBS, 50 µL of peroxidase-labeled anti-digoxigenin were added on the slides and incubated at 37 °C for 30 min away from the light. Finally, a diamidino-2-phenylindole (DAPI) solution was added dropwisely onto the slides at room temperature and incubated for 10 min before the slides were observed under a fluorescence microscope. The nuclei showing a green color were considered as apoptotic cells, while the nuclei showing a blue color were considered as normal cells. A total of 10 visual fields were selected randomly to calculate the apoptotic index.

### **Statistical analysis**

Statistical analysis was performed using SPSS16.0 statistical software. The measurement data were presented by mean values and standard deviation, while the average values between two groups were compared using t-tests. The comparison between multiple groups were conducted using one way ANOVA followed by the Scheffé's method as the post hoc text. A P value of < 0.05 was considered statistically significant.

## **Results**

## **MT enhanced H19 expression via promoting the transcription efficiency of H19 promoter**

Real-time PCR and luciferase assay were performed to detect the effect of MT on H19 expression after various doses of MT (1  $\mu$ M and 10  $\mu$ M) were utilized to treat U251 and SH-SY5Y cells. As shown in Fig. 1, the H19 level in U251 (Fig. 1A) and SH-SY5Y (Fig. 1B) cells treated with MT was up-regulated in a dose-dependent manner. Subsequently, a luciferase assay was performed to explore the underlying mechanism of MT effect on H19 expression. The results showed that the luciferase activity of H19 promoter in U251 (Fig. 1C) and SH-SY5Y (Fig. 1D) cells was increased in a dose-dependent manner after MT treatment, indicating that MT enhanced H19 expression via promoting the transcription efficiency of H19 promoter.

## **HIF1A was a virtual target gene of miR-675**

To identify the potential target gene of miR-675, we searched an online microRNA database ([www.mirdb.org](http://www.mirdb.org)) and found that HIF1A was a potential target gene of miR-675 with a miR-675 binding site located in HIF1A 3'UTR (Fig 2A). Subsequently, a dual-luciferase assay was used to confirm that HIF1A was indeed a target gene of miR-675. As shown in Fig. 2, the luciferase activity of U251 (Fig. 2B) and SH-SY5Y (Fig. 2C) cells transfected with wild-type HIF1A 3'UTR and miR-675 mimics was significantly lower than those cells transfected with the scramble control, while the transfection of miR-675 mimics showed no effect on the luciferase activity of mutant HIF1A 3'UTR, suggesting that HIF1A was a direct target gene of miR-675. The interaction between miR-675 and HIF1A was further investigated in U251 (Fig.2D) and SH-SY5Y (Fig.2E) cells transfected with HIF1A constructs, in which reduced luciferase activity of miR-675 promoter was observed compared with transfection of negative controls. In addition, the transfection with HIF1A constructs inhibited miR-675 expression in U251 (Fig. 2F) and SH-SY5Y (Fig. 2G) cells, validating that miR-675 and HIF1A mutually inhibited the expression of each other.

## **HIF1A enhanced TLR4 expression via promoting the transcription efficiency of TLR4 promoter**

Real-time PCR and luciferase assay were performed to detect the effect of HIF1A on TLR4 expression. As shown in Fig. 3, the transfection of HIF1A constructs up-regulated the luciferase activity of TLR4 promoter in U251 (Fig. 3A) and SH-SY5Y (Fig. 3B) cells. In addition, the transfection of HIF1A constructs enhanced TLR4 expression in U251 (Fig. 3C) and SH-SY5Y (Fig. 3D) cells, validating the fact that HIF1A enhanced TLR4 expression by promoting the transcription efficiency of TLR4 promoter.

## **Effect of MT on the expression of miR-675, HIF1A and TLR4**

MiR-675, HIF1A and TLR4 expression were determined in U251 (Fig. 4A-4D) and SH-SY5Y (Fig. 4E-4H) cells after treatment with various doses of MT (1  $\mu$ M and 10  $\mu$ M). As shown in Fig. 4, MT dose-dependently increased miR-675 (Fig. 4A and 4E) expression, but reduced the mRNA levels of HIF1A (Fig. 4B and 4F) and TLR4 (Fig. 4C and 4H) in U251 (Fig. 4A, B and C) and SH-SY5Y (Fig. 4E, F and G) cells. In addition, MT treatment also reduced the protein levels of HIF1A and TLR4 (Fig. 4D and 4H) in U251 (Fig. 4D) and SH-SY5Y (Fig. 4H) cells.

## **MT attenuated SAH-induced neurobehavioral deficits and apoptosis**

Daily neurobehavioral testing was carried out at the baseline (before the onset of SAH) and after the onset of SAH using a neurological score test. As shown in Fig. 5A, vehicle-treated C57BL/6J mice experienced significant neurobehavioral deficits after the onset of SAH, while MT-treated C57BL/6J mice displayed significantly less neurobehavioral deficits. In addition, the extent of cell apoptosis (Fig. 5B and 5C) was the lowest in the sham group and the highest in the SAH group. The severity of SAH in each SAH-involved group was comparable (data not shown).

## **Differential expression of H19, miR-675, HIF1A and TLR4 among various groups**

IHC assays were performed to measure the protein levels of HIF1A and TLR4 among sham, SAH, and SAH+MT groups. As shown in Fig. 6 and 7, HIF1A (Fig. 6) and TLR4 (Fig. 7) protein levels were the highest in the SAH group and the lowest in the sham group. Subsequently, real-time PCR and Western-blot analysis were also utilized to measure the levels of H19, miR-675, HIF1A and TLR4 among sham, SAH, and SAH+MT groups. As shown in Fig. 8, the mRNA levels of H19 (Fig. 8A) and miR-675 (Fig. 8B) were the lowest in the SAH group and the highest in the sham group. On the contrary, the levels of HIF1A (Fig. 8C, 8E) and TLR4 (Fig. 8D, 8E) were the highest in the SAH group and the lowest in the sham group. To sum up, the molecular mechanisms underlying the therapeutic effect of MT in the management of post-SAH DBI can be explained as Fig.9, in which MT could up-regulate the expression of H19, whose chromosomal segment hosted miR-675. And HIF1A, which is also a target gene of miR-675, could induce the expression of TLR4, which played an important role in the release of pro-inflammatory cytokines such as TNF- $\alpha$  and interleukins. Inflammatory factors are involved in cell apoptosis, which is a significant manifestation of post-SAH DBI.

## **Discussion**

As a type of indolamine, MT is derived from tryptophan and has a high biological availability upon entering brain parenchyma [26]. Previous articles have demonstrated that MT exerts protective effects against post-SAH EBI in rats [27, 28]. In addition, MT can be beneficial in alleviating EBI, and thus can exert a protective function in the treatment of SAH [29]. Furthermore, MT was also shown to reduce neuronal apoptosis, decrease mortality, and prevent vasospasm [30]. It was also demonstrated that MT could reduce focal cerebellum injury [31]. Moreover, the application of MT been also found that administration of MT could alter the expression of lncRNA and H19, and H19 has been shown to host miR-675, and miR-675 has been found to be a negative regulator of P53 [27, 32]. A previous study also demonstrated that MT treatment could protect against post-SAH EBI by mediating the functions of H19-let-7a-NGF-apoptosis and H19-miR-675-P53-apoptosis signaling pathways [11, 32]. And the carcinogenesis function of H19, which was identified as a miR-675 precursor, is also mediated by miR-675 [33]. In this study, we detected the effect of MT on H19 expression and found that MT enhanced H19 expression via promoting the transcription efficiency of H19 promoter. And we also demonstrated that MT could enhance the expression of miR-675.

It has been shown that the reduced expression of miR675-5p under low O<sub>2</sub> partial pressure could inhibit hypoxic responses by reducing the expression of nuclear HIF-1 $\alpha$  and miR675-5p [34]. In this study, we investigate the interaction between miR-675 and HIF1A, and found that miR-675 was directly bound to HIF1A, while the inhibitory effect between miR-675 and HIF1A were mutual. Subsequently, MT treatment also validated the interaction between miR-675 and HIF1A via inhibiting expression of HIF1A mRNA and protein while promoting expression of miR-675.

Interestingly, as the most frequently studied  $\alpha$  subunit, stabilized HIF1A can migrate to the nuclei upon the reduction of oxygen tension. In the nuclei, HIF1A binds to ARNT/HIF1B and produce HIF1, which in turn interacts with hypoxic response elements to increase the expression of various genes and hence maintain the homeostasis in the body [35]. It is now recognized that both the accumulation of HIF1A and the transcriptional activation of HIF1 can be induced by inflammatory conditions and lipo-polysaccharide challenge [36]. In this study, we evaluated the effect of HIF1A on TLR4 expression, and found that HIF1A enhanced TLR4 expression via promoting the transcription efficiency of TLR4 promoter.

Moreover, as an important component of innate immunity, TLR4 plays an important role in the initiation of several signaling pathways, such as the release of NF- $\kappa$ B, and multiple proinflammatory mediators, including TNF- $\alpha$ , IL-8, IL-1 $\beta$  and IL-6 [37]. Kim et al. found that the presence of CoCl<sub>2</sub> and severe hypoxia could increase TLR4 expression in macrophages [38]. In fact, as a well-studied pattern-recognition receptor (PRR), TLR can recruit specific adaptor molecules containing the TIR domain, including TRIF and MyD88, and initiate a series of signaling events such as the release of NF- $\kappa$ B and relevant cytokines [39]. In addition, TLR4 can interact with MyD88 and TIR-domain-containing adapter-inducing interferon- $\beta$  (TRIF) to activate the NF- $\kappa$ B pathway, which in turn mediates the expression of inflammatory factors including IL-1 $\alpha$  and IL-1 $\beta$ , IL-6 and TNF- $\alpha$  [40]. Previously, it has also been shown that TLR4 could lead to inflammatory injuries in the central nervous system during cerebral ischemia and infection [6]. In this study, we observed ameliorated neuro deficits and reduced apoptosis index along with inhibited TLR4 expression in the SAH animal models.

Inflammatory resolution is increasingly viewed as a process participated by multiple important mediators, and its dysregulation can lead to the onset of many chronic inflammatory diseases [41]. Apoptosis is shown to play a crucial function to maintain a normal state of inflammatory responses, whereas the dysregulation of inflammatory responses can be induced by an increased amount of reactive oxygen species (ROS), whose synthesis may also lead to excessive apoptosis [42]. While the cellular events involved in keeping a constant number of Leydig cells have not been clearly understood yet, apoptosis has been thought to play a critical function in the regulation of Leydig cells. In this study, MT treatment was shown to reduce miR-675 expression, while increasing the expression of HIF1A and TLR4. Furthermore, when treated with MT, the elevated HIF1A and TLR4 levels in SAH rats were partly restored.

## Conclusion

We firstly found that MT regulated HIF1A expression and ameliorated post-SAH DBI via the signaling pathway of H19/miR-675/HIF1A/TLR4. MT has also been found to up-regulate the expression of H19, whose chromosomal segment hosted miR-675. Furthermore, HIF1A was found to be a target gene of miR-675 and induced the expression of TLR4, which played an important role in the release of pro-inflammatory cytokines such as TNF- $\alpha$  and interleukins. Moreover, inflammatory factors are involved in cell apoptosis, a significant manifestation of post-SAH DBI.

## Abbreviations

HIF1A

hypoxia-inducible factor 1 $\alpha$ ;

DBI

delayed brain injury;

SAH

subarachnoid hemorrhage;

IHC

immunohistochemistry;

EBI

early brain injury;

TLR4

toll-like receptor 4;

NF- $\kappa$ B

nuclear factor kappa B;

MyD88

myeloid differentiation factor 88;

TNF

tumor necrosis factor;

MMP

matrix metalloproteinase;

ICAM

intercellular adhesion molecule;

MCP

monocyte chemo-attractant protein;

lncRNA

long non-coding RNA;

MT

melatonin;

HIF1A

hypoxia-inducible factor 1 $\alpha$ ;

FCS

fetal calf serum;

WT

wild type;

TBST

Tris-Buffered Saline and Tween 20;

SP

streptavidin-peroxidase;

## **Declarations**

### **Ethics approval and consent to participate**

All experiments were carried out under NIH 's Guide for the Care and Use of Laboratory Animals and were approved by the Ethics Committee of our institute.

### **Consent for publication**

Not applicable

### **Competing interests**

None

### **Funding**

The study was sponsored by Natural Science Research Project of Higher Education of Anhui Province (Project No. KJ2018A0253)

### **Authors' contributions**

DX and SY planned the study, XJ and ZL collected the literature, DX, XJ, ZL and YD collected and analyzed the data, ZZ and SY visualized the data, DX and SY composed the manuscript, and all the other co-authors approved the final manuscript.

### **Acknowledgements**

Not applicable

## Availability of data and material

The data that support the findings of this study are available from the corresponding author upon reasonable request.

## References

1. Listed, N.: Epidemiology of aneurysmal subarachnoid hemorrhage in Australia and New Zealand: incidence and case fatality from the Australasian Cooperative Research on Subarachnoid Hemorrhage Study (ACROSS). *Stroke* 2000;31:1843-1850.
2. Suzuki, H.: What is early brain injury? *Transl Stroke Res* 2015;6:1-3.
3. Kawakita, F., et al.: Effects of Toll-Like Receptor 4 Antagonists Against Cerebral Vasospasm After Experimental Subarachnoid Hemorrhage in Mice. *Mol Neurobiol* 2017;54:6624-6633.
4. Hanafy, KA.: The role of microglia and the TLR4 pathway in neuronal apoptosis and vasospasm after subarachnoid hemorrhage. *J Neuroinflammation* 2013;10:83.
5. Wang, Z., et al.: Progesterone administration modulates cortical TLR4/NF-kappaB signaling pathway after subarachnoid hemorrhage in male rats. *Mediators Inflamm* 2011;2011:848309.
6. Buchanan, MM., Hutchinson, M., Watkins, LR., Yin, H.: Toll-like receptor 4 in CNS pathologies. *J Neurochem* 2010;114:13-27.
7. Bartel, DP.: MicroRNAs: genomics, biogenesis, mechanism, and function. *Cell* 2004;116:281-297.
8. Hwang, HW., Mendell, JT.: MicroRNAs in cell proliferation, cell death, and tumorigenesis. *Br J Cancer* 2006;94:776-780.
9. Gupta, RA., et al.: Long non-coding RNA HOTAIR reprograms chromatin state to promote cancer metastasis. *Nature* 2010;464:1071-1076.
10. Galano, A., Tan, DX., Reiter, RJ.: On the free radical scavenging activities of melatonin's metabolites, AFMK and AMK. *J Pineal Res* 2013;54:245-257.
11. Yang, S., et al.: Long non-coding RNA and microRNA-675/let-7a mediates the protective effect of melatonin against early brain injury after subarachnoid hemorrhage via targeting TP53 and neural growth factor. *Cell Death Dis* 2018;9:99.
12. Barchas, J., DaCosta, F., Spector, S.: Acute pharmacology of melatonin. *Nature* 1967;214:919-920.
13. Beni, SM., Kohen, R., Reiter, RJ., Tan, DX., Shohami, E.: Melatonin-induced neuroprotection after closed head injury is associated with increased brain antioxidants and attenuated late-phase activation of NF-kappaB and AP-1. *FASEB J* 2004;18:149-151.
14. Pei, Z., Fung, PC., Cheung, RT.: Melatonin reduces nitric oxide level during ischemia but not blood-brain barrier breakdown during reperfusion in a rat middle cerebral artery occlusion stroke model. *J*

Pineal Res 2003;34:110-118.

15. Cai, B., et al: Long noncoding RNA H19 mediates melatonin inhibition of premature senescence of c-kit(+) cardiac progenitor cells by promoting miR-675. *J Pineal Res* 2016;61:82-95.
16. Liu, C., Chen, Z., Fang, J., Xu, A., Zhang, W., Wang, Z.: H19-derived miR-675 contributes to bladder cancer cell proliferation by regulating p53 activation. *Tumour Biol* 2016;37:263-270.
17. Sehba, F. A., Hou, J., Pluta, R. M., Zhang, J. H. The importance of early brain injury after subarachnoid hemorrhage. *Prog Neurobiol* 2012; 97:14–37.
18. Yang, S., Tang, W., He, Y., Wen, L., Sun, B., Li, S.: Long non-coding RNA and microRNA-675/let-7a mediates the protective effect of melatonin against early brain injury after subarachnoid hemorrhage via targeting tp53 and neural growth factor. *Cell Death Dis* 2018;9(2):99.
19. Wang, R., Zhou, S., Wu, P., Li, M., Ding, X., & Sun, L., et al.: Identifying involvement of h19-mir-675-3p-igf1r and h19-mir-200a-pdcd4 in treating pulmonary hypertension with melatonin. *Mol Ther Nucleic Acid* 2018;13:44-54.
20. Costa, V., et al.: Hypoxia-inducible factor 1Alpha may regulate the commitment of mesenchymal stromal cells toward angio-osteogenesis by mirna-675-5P. *Cytotherapy* 2017;19:1412-1425.
21. Schwartz, A. Y., et al.: Experimental models of subarachnoid hemorrhage in the rat: a refinement of the endovascular filament model. *J Neurosci Methods* 2000;96(2):161-167.
22. Milner, E., et al.: HIF-1 $\alpha$  Mediates Isoflurane-Induced Vascular Protection in Subarachnoid Hemorrhage. *Ann Clin Transl Neurol* 2015;2:325-337.
23. Cao, S. , et al.: Melatonin-mediated mitophagy protects against early brain injury after subarachnoid hemorrhage through inhibition of nlrp3 inflammasome activation. *Sci Rep* 2017;7(1): 2417.
24. Vellimana, A. K., et al.: Endothelial Nitric Oxide Synthase Mediates Endogenous Protection Against Subarachnoid Hemorrhage-Induced Cerebral Vasospasm. *Stroke* 2011; 42:776-782.
25. Livak K.J., Schmittgen T.D.. Analysis of relative gene expression data using real-time quantitative PCR and the 2(-Delta Delta C(T)). *Method. Methods* 2001;25(4):402–8.
26. Tordjman, S., et al.: Melatonin: Pharmacology, Functions and Therapeutic Benefits. *Curr Neuropharmacol* 2017;15:434-443.
27. Wang, Z., et al.: Melatonin activates the Nrf2-ARE pathway when it protects against early brain injury in a subarachnoid hemorrhage model. *J Pineal Res* 2012;53:129-137.
28. Yang, GY., Betz, AL., Chenevert, TL., Brunberg, JA., Hoff, JT.: Experimental intracerebral hemorrhage: relationship between brain edema, blood flow, and blood-brain barrier permeability in rats. *J Neurosurg* 1994;81:93-102.
29. Keniry, A., et al.: The H19 lincRNA is a developmental reservoir of miR-675 that suppresses growth and Igf1r. *Nat Cell Biol* 2012;14:659-665.
30. Gao, Y., et al.: The H19/let-7 double-negative feedback loop contributes to glucose metabolism in muscle cells. *Nucleic Acids Res* 2014;42:13799-13811.

31. Ersahin, M., et al.: Melatonin reduces experimental subarachnoid hemorrhage-induced oxidative brain damage and neurological symptoms. *J Pineal Res* 2009;46:324-332.
32. Martinez-Cruz, F., Espinar, A., Pozo, D., Osuna, C., Guerrero, JM.: Melatonin prevents focal rat cerebellum injury as assessed by induction of heat shock protein (HO-1) following subarachnoid injections of lysed blood. *Neurosci Lett* 2002;331:208-210.
33. Matouk, IJ., Halle, D., Gilon, M., Hochberg, A.: The non-coding RNAs of the H19-IGF2 imprinted loci: a focus on biological roles and therapeutic potential in Lung Cancer. *J Transl Med* 2015;13:113.
34. Lo Dico, A., et al.: MiR675-5p Acts on HIF-1alpha to Sustain Hypoxic Responses: A New Therapeutic Strategy for Glioma. *Theranostics* 2016;6:1105-1118.
35. Semenza GL: Oxygen sensing, homeostasis, and disease. *N Engl J Med* 2011;365:537-547.
36. Richard, DE., Berra, E., Pouyssegur, J.: Nonhypoxic pathway mediates the induction of hypoxia-inducible factor 1alpha in vascular smooth muscle cells. *J Biol Chem* 2000;275:26765-26771.
37. Akira, S., Uematsu, S., Takeuchi, O.: Pathogen recognition and innate immunity. *Cell* 2006;124:783-801.
38. Kim, SY., et al.: Hypoxic stress up-regulates the expression of Toll-like receptor 4 in macrophages via hypoxia-inducible factor. *Immunology* 2010;129:516-524.
39. Kawai, T., Akira, S.: The role of pattern-recognition receptors in innate immunity: update on Toll-like receptors. *Nat Immunol* 2010;11:373-384.
40. Miyake, K.: Endotoxin recognition molecules MD-2 and toll-like receptor 4 as potential targets for therapeutic intervention of endotoxin shock. *Curr Drug Targets Inflamm Allergy* 2004;3:291-297.
41. Shores, DR., Binion, DG., Freeman, BA., Baker, PR.: New insights into the role of fatty acids in the pathogenesis and resolution of inflammatory bowel disease. *Inflamm Bowel Dis* 2011;17:2192-2204.
42. Oyinloye, BE., Adenowo, AF., Kappo, AP.: Reactive oxygen species, apoptosis, antimicrobial peptides and human inflammatory diseases. *Pharmaceuticals (Basel)* 2015;8:151-175.

## Figures

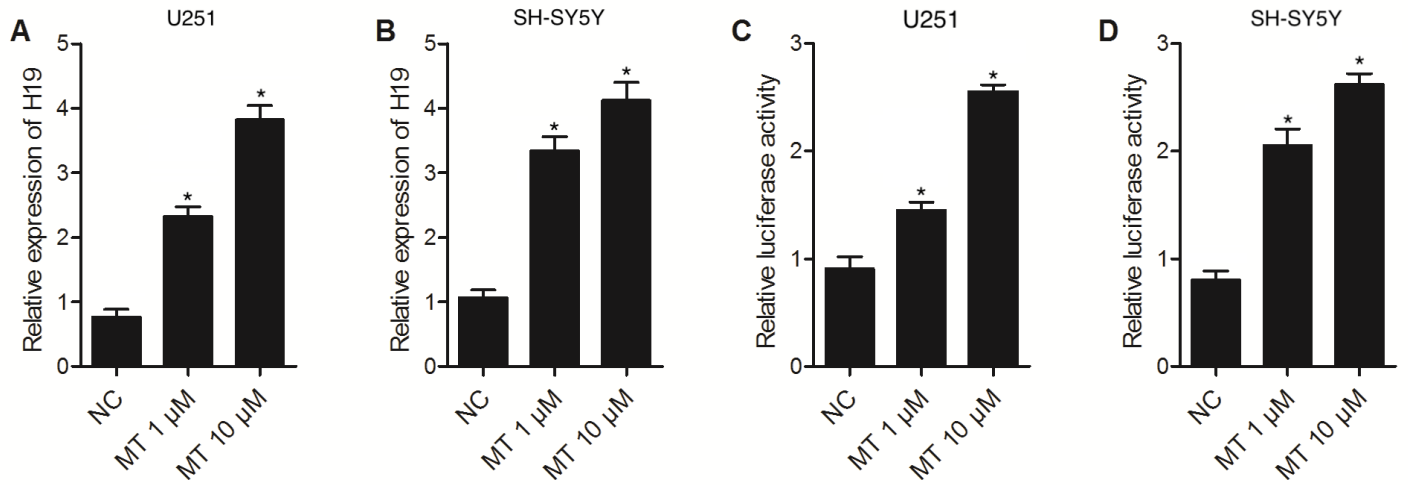


**Figure 1**

MT enhanced H19 expression via promoting the transcription efficiency of H19 promoter A: MT dose-dependently increased H19 level in U251 cells (\* P value < 0.05, vs. NC; NC: negative control group) B: MT dose-dependently increased H19 level in SH-SY5Y cells (\* P value < 0.05, vs. NC; NC: negative control group) C: MT dose-dependently increased the luciferase activity of H19 promoter in U251 cells (\* P value < 0.05, vs. NC; NC: negative control group) D: MT dose-dependently increased the luciferase activity of H19 promoter in SH-SY5Y cells (\* P value < 0.05, vs. NC; NC: negative control group)



the luciferase activity of miR-675 promoter in U251 cells (\* P value < 0.05, vs. pcDNA group) E: Transfection with HIF1A constructs reduced the luciferase activity of miR-675 promoter in SH-SY5Y cells (\* P value < 0.05, vs. pcDNA group) F: MiR-675 level in U251 cells was down-regulated subsequent to transfection with HIF1A plasmids (\* P value < 0.05, vs. pcDNA group) G: MiR-675 level in SH-SY5Y cells was down-regulated subsequent to transfection with HIF1A plasmids (\* P value < 0.05, vs. pcDNA group)

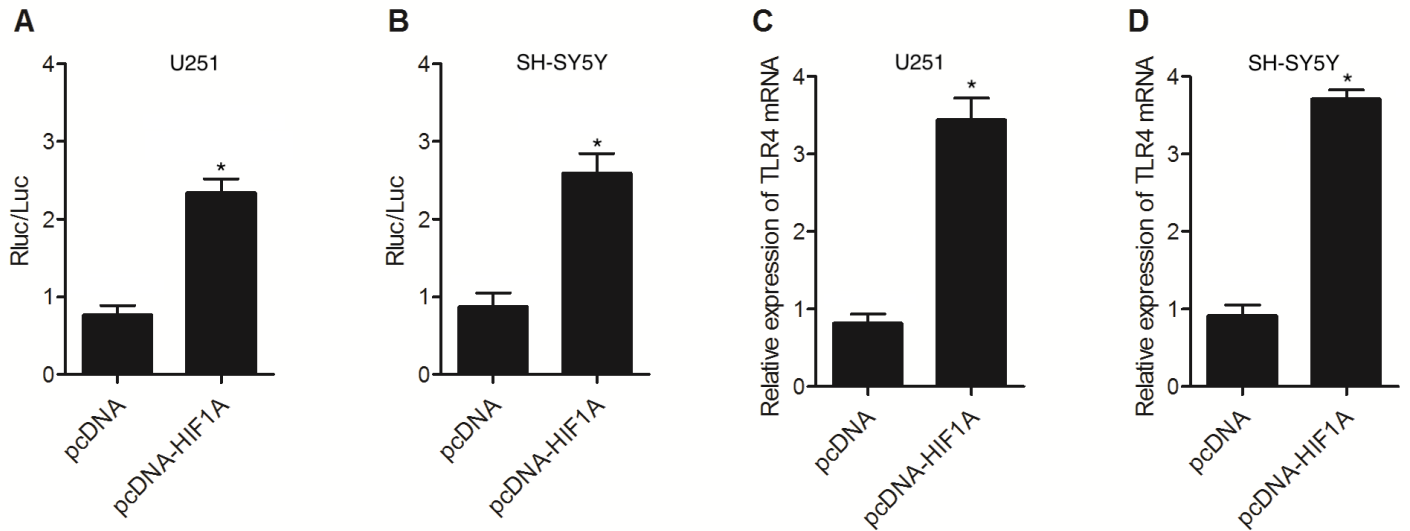


**Figure 3**

HIF1A enhanced TLR4 expression via promoting the transcription efficiency of TLR4 promoter A: Transfection with HIF1A constructs reduced the luciferase activity of TLR4 promoter in U251 cells (\* P value < 0.05, vs. pcDNA group) B: Transfection with HIF1A constructs reduced the luciferase activity of TLR4 promoter in SH-SY5Y cells (\* P value < 0.05, vs. pcDNA group) C: TLR4 level in U251 cells was down-regulated subsequent to transfection with HIF1A plasmids (\* P value < 0.05, vs. pcDNA group) D: TLR4 level in SH-SY5Y cells was down-regulated subsequent to transfection with HIF1A plasmids (\* P value < 0.05, vs. pcDNA group)

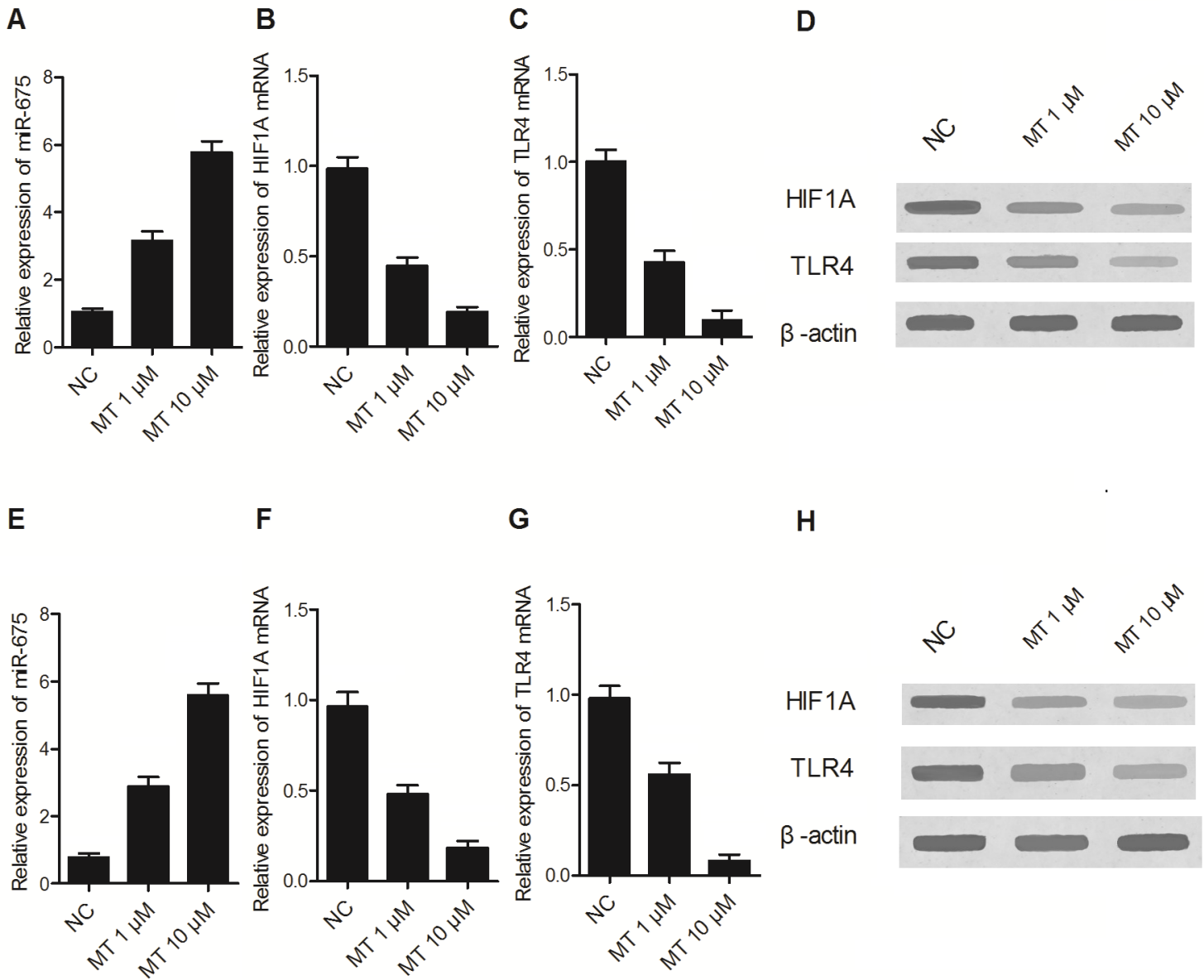


**Figure 4**

The effect of MT on the expression of miR-675, HIF1A and TLR4 A: Treatment with MT elevated miR-675 level in U251 cells (\* P value< 0.05, vs. NC; NC: negative control group) B: The level of HIF1A mRNA in U251 cells was significantly decreased after MT treatment (\* P value< 0.05, vs. NC; NC: negative control group) C: The level of TLR4 mRNA in U251 cells was significantly decreased after MT treatment (\* P value< 0.05, vs. NC; NC: negative control group) D: HIF1A and TLR4 protein levels in U251 cells was down-regulated following MT treatment E: Treatment with MT elevated miR-675 level in SH-SY5Y cells (\* P value< 0.05, vs. NC; NC: negative control group) F: The level of HIF1A mRNA in SH-SY5Y cells was significantly decreased after MT treatment (\* P value< 0.05, vs. NC; NC: negative control group) G: The level of TLR4 mRNA in SH-SY5Y cells was significantly decreased after MT treatment (\* P value< 0.05, vs. NC; NC: negative control group) H: HIF1A and TLR4 protein levels in SH-SY5Y cells was down-regulated following MT treatment

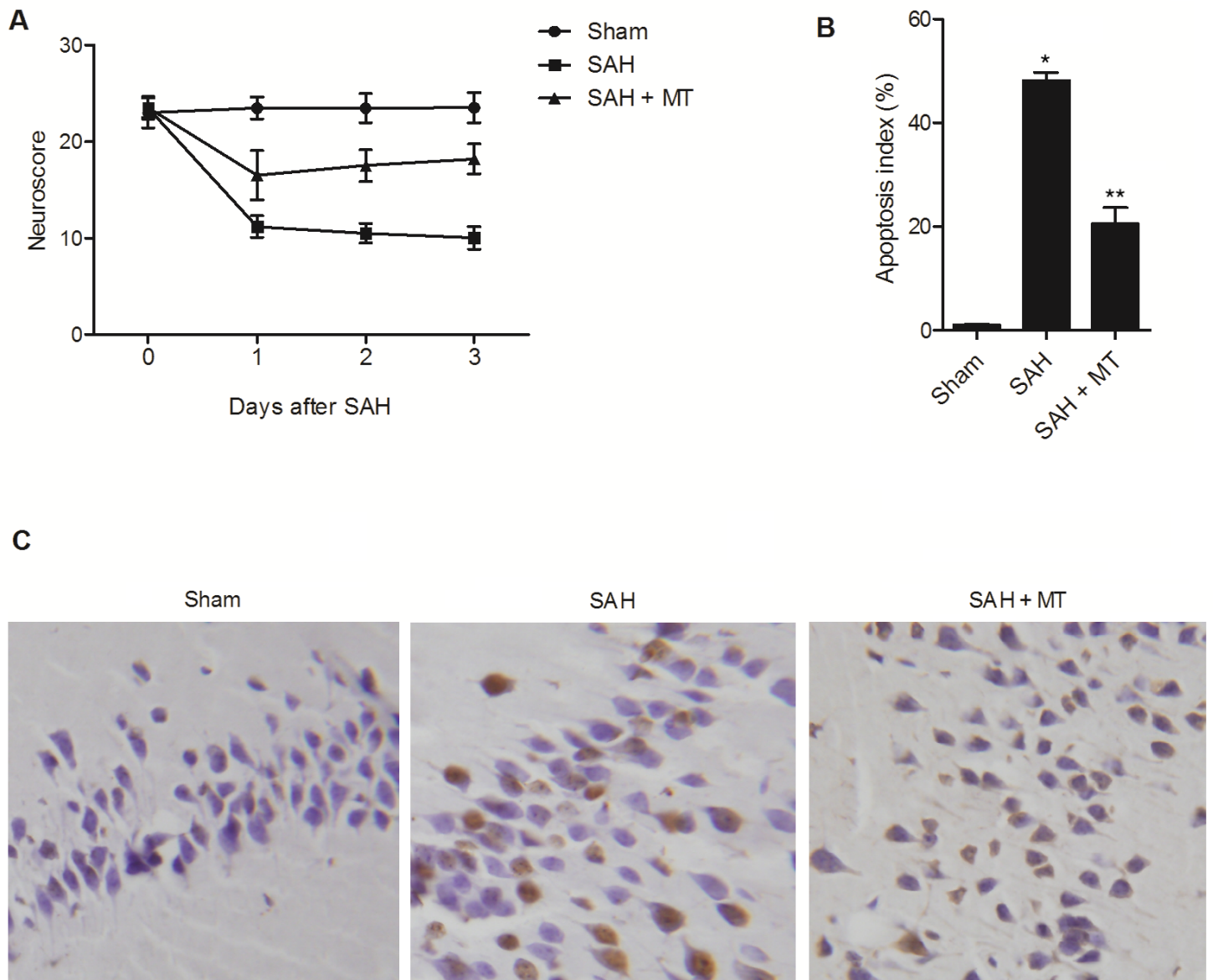


**Figure 5**

MT attenuated SAH-induced neurobehavioral deficits and apoptosis A: MT attenuated neurobehavioral deficits induced by SAH B/C: The extent of cell apoptosis in the SAH+MT group was much higher than that in the sham group, while the extent of cell apoptosis was the highest in the SAH group (Scale bar: 10  $\mu$ m; \* P value < 0.05, vs. sham group; \*\* P value < 0.05, vs. SAH group).

Sham

SAH

SAH + MT

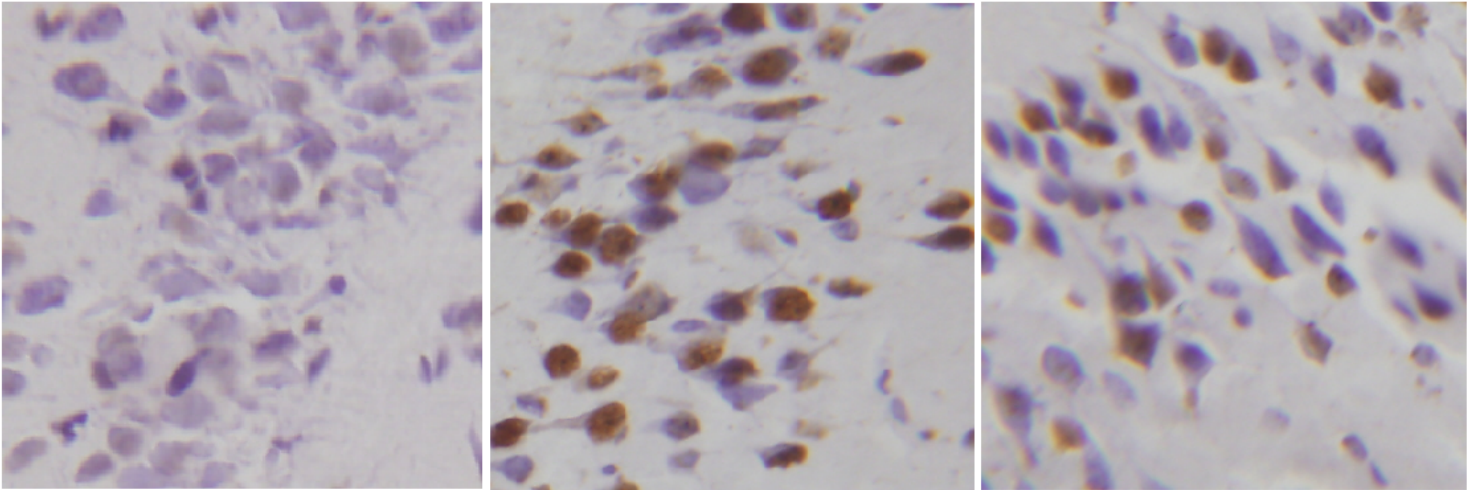


**Figure 6**

HIF1A protein level was the lowest in the sham group and the highest in the SAH group (Scale bar: 10 um).

Sham

SAH

SAH + MT

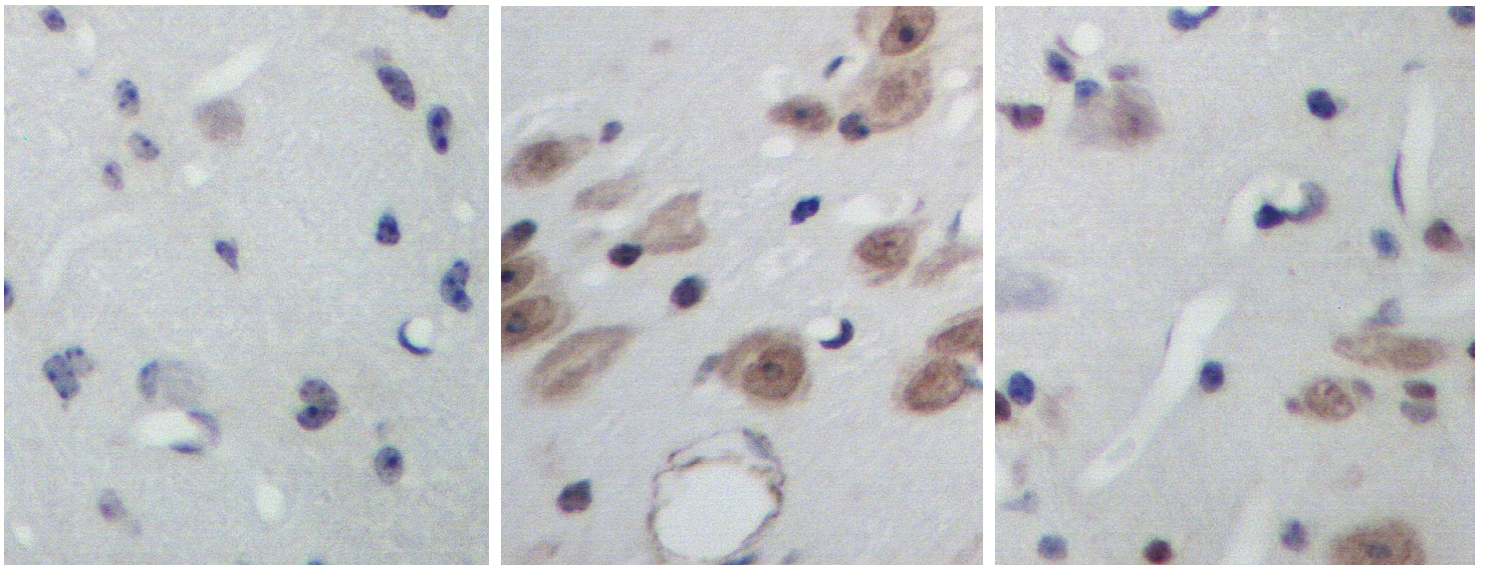


**Figure 7**

TLR4 protein level was the lowest in the sham group and the highest in the SAH group (Scale bar: 10 um).

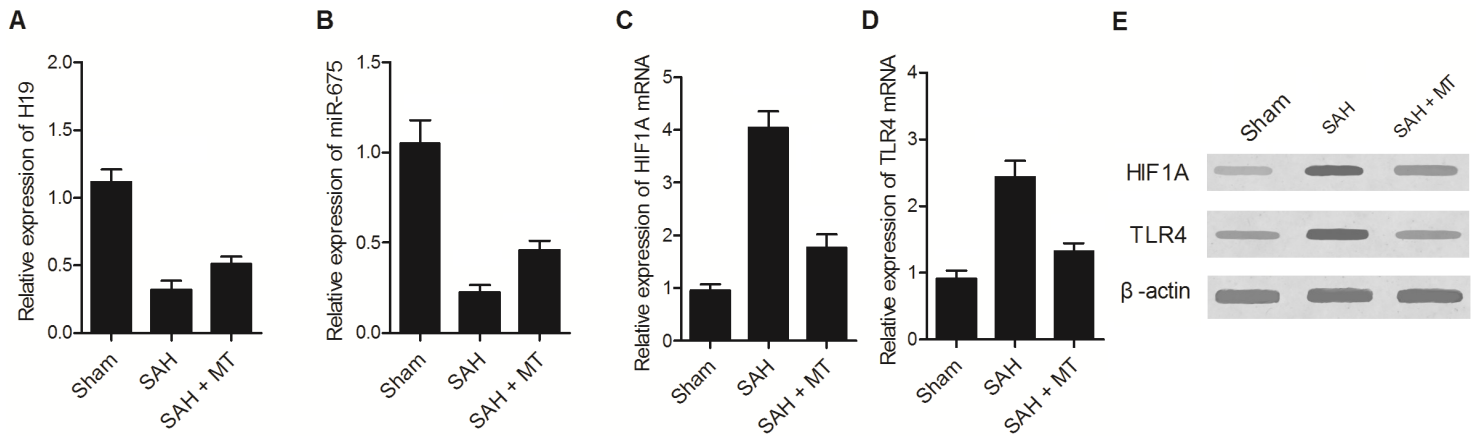


**Figure 8**

Differential expression of H19, miR-675, HIF1A and TLR4 among various groups A: H19 mRNA level was the highest in the sham group and the lowest in the SAH group (\* P value < 0.05, vs. sham group; \*\* P value < 0.05, vs. SAH group) B: miR-675 level was the highest in the sham group and the lowest in the SAH group (\* P value < 0.05, vs. sham group; \*\* P value < 0.05, vs. SAH group) C: HIF1A protein level was the lowest in the sham group and the highest in the SAH group (\* P value < 0.05, vs. sham group; \*\* P value < 0.05, vs. SAH group) D: TLR4 mRNA level was the lowest in the sham group and the highest in the SAH group (\* P value < 0.05, vs. sham group; \*\* P value < 0.05, vs. SAH group) E: Protein levels of HIF1A and TLR4 were the lowest in the sham group and the highest in the SAH group.

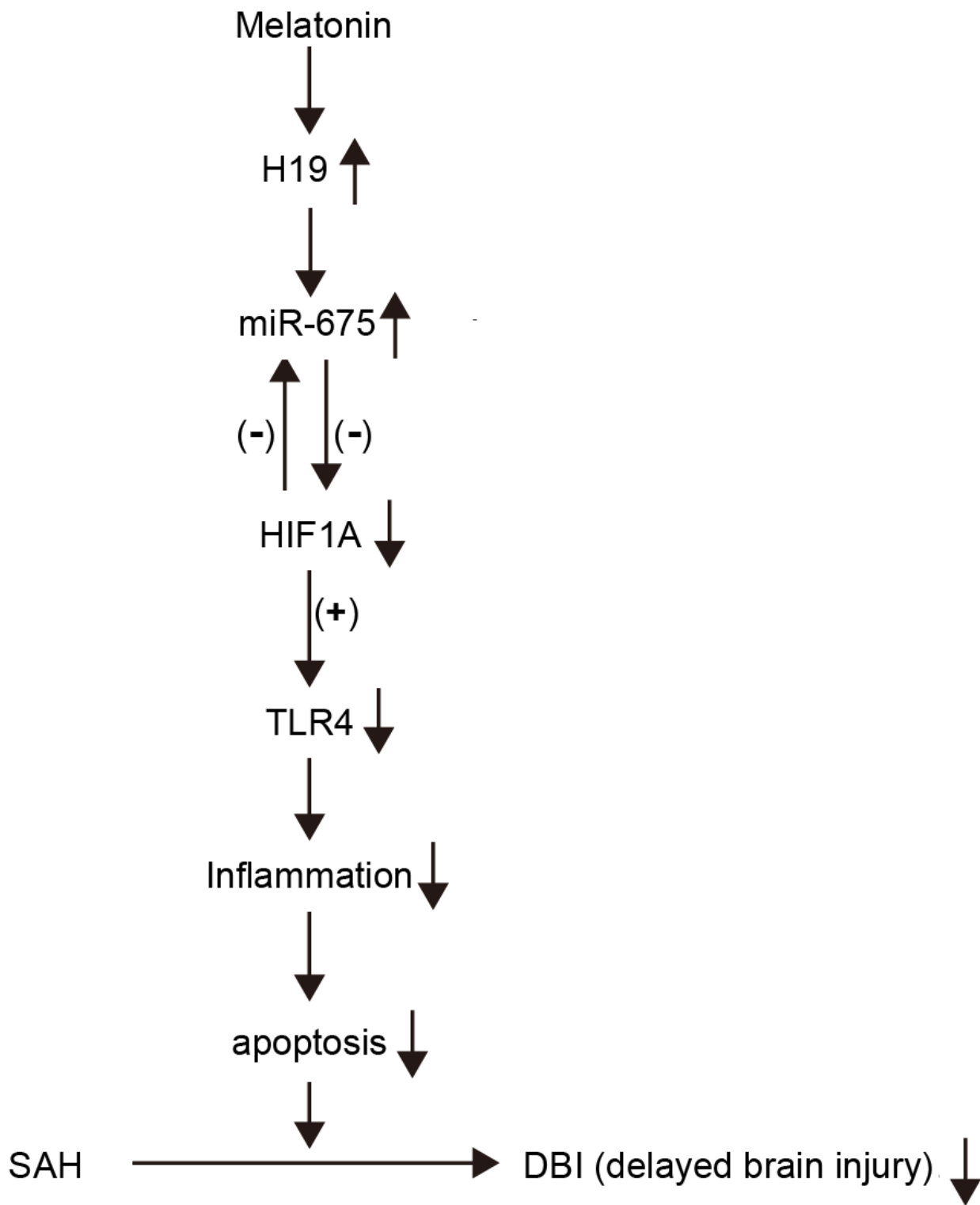


Figure 9

The molecular mechanisms underlying the therapeutic effect of MT in the management of post-SAH DBI.